INTERNATIONAL JOURNAL OF RESEARCH
In Advanced Engineering Technologies

Volume 3, Issue 1 OCT 2014

OPERATION OF 3-PHASE POWER CONVERTER CONNECTED TO A DISTRIBUTION SYSTEM WITH PHOTOVOLTAIC SYSTEM

N UMAKAMESHWARI DEEPIKA

P.G. scholar, Dept of EEE, Vignan Bharathi Institute of Technology

Mail id: deepika.sriganesh@gmail.com

J. ARCHANA

Asst. professor,Dept of EEE, Vignan Bharathi Institute of Technology

Mail id:archanaanu.403@gmail.com

ABSTRACT--This paper presents the operation of a 3-phase power connected to a distributed generation (DG) system with photovoltaic system. Distributed generation (DG) system driven by a dc-dc step-up converter and a dc-ac voltage source inverter (VSI) interfaced with the power grid. To create a stable mode when different kinds of loads are connected locally or when working under contingency, the step-up converter must regulate the dc link voltage, allowing the VSI to stabilize its terminal voltage. PI controller is used to regulate voltages and currents, while a phase-locked loop algorithm is used to synchronize the grid and DG.

I. INTRODUCTION

RECENTLY, due to the high price of oil and the concern forthe environment, renewable energy is in the limelight. Thisscenario has stimulated the development of alternative powersources such as photovoltaic panels, wind turbines and fuelcells [1]–[3]. Amongrenewable energy systems, photovoltaic (PV) systems areexpected to play an important role in the future and, as such,a great deal of research effort is dedicated to enhancing theirperformance and efficiency at the component and system levels.As two influential factors in regards to the performance and efficiencyof a PV system, the impact of characteristic mismatchesamongst PV cells and the phenomenon of maximum-powerdrop due to partial shading have been the subject of intenseresearch.

The distributed generation (DG) concept emergedas a way to integrate different power plants, increasing the DGowner's reliability, reducing emissions, and providing

to command the voltage source inverter (VSI) additionalpower quality benefits [4]. The cost of the distribution powergeneration system using the renewable energies is on a fallingtrend and is expected to fall further as demand and production increase.The energy sources used in DG systems usually have different output characteristics, and for this reason, power electronic converters are employed to connect these energy sources to the grid.In a PV system, PV modules are connected in series and inparallel in order to enable power generation and processing atan adequately large voltage level and efficiency. However, whenPV cells in a module are shaded, they experience a significantpower output drop and can even act as loads to other (unshaded)cells and modules. This phenomenon can result in hot-spot formationin, and potential damage of, the shaded cell(s), in additionto a disproportionate maximum-power drop in the overallarray.

The use of distributed generation (DG) sources is currently being considered as a solution to the growing problems of energy demand . Apart from the consequent reduction in the size of the generating plants and the possibility of modular implementation, DG systems based on renewable energy sources [2] (photovoltaic, fuel cells, and storage systems such as ultra-capacitors and batteries) are of great interest due to their low environmental impact [3] and technical advantages such as improvements in voltage levels and reduced power losses when a DG system is installed in radial lines [4]. DG systems also promote cogeneration [5] and improve overall system efficiency [6].

Recently, the use of power or current in the d-q synchronous reference frame [11]–[14] as control variables

connected to the grid has generated considerable interest from the scientific community. With either method, before or after the contingency takes place, the control variable remains the same, making the DG operate with limited capability to supply the load.

On the other hand, two control algorithms were proposed to improve the grid-connected and intentional-islanding operations methods in [15], in which the DG system must detect the situation and switch from power or current to voltage as a control variable to provide constant rms voltage to the local loads.

In [16] and [17], the power flow is determined by controlling the amplitude and angle of displacement between the voltage produced by the DG and the grid voltage [18], i.e., the control variable is the same before and after the islanding mode occurs.

The voltage control provides the capability to supply different kinds of loads to the DG system, such as linear, nonlinear, and motor, balanced, or unbalanced [19], even if the DG operates in the islanding mode. These kinds of controls are suitable for DGs operating in parallel as each of the DGs are connected to the grid through a distribution transformer (DT) [20]. Conversely, the other approaches introduced in [21], [22] are more effective. This paper analyzes the effects caused by 50 to 5000-kVA DG sources inserted into the distribution system, whether the local load is linear or nonlinear, or if the grid is operating under abnormal conditions. Section II details the method used to drive both converters. Section III discusses the technique to control the power flow through the grid. Sections IV and V show the simulation setup to confirm the previous analysis, while the main points presented in this paper appear in the conclusion.

II.PV SYSTEM DESCRIPTION AND MODELING

A PV generator is a combination of solar cells, connections, protective parts, supports, etc. In the present modeling, the focus is only on cells. Solar cells consist of a p-n junction. Thus, the simplest equivalent circuit of a solar cell is a current source in parallel with a diode.

The output of the current source is directly proportional to the light falling on the cell (photocurrent). During darkness, the solar cell is not an active device; it works as a diode, i.e., a p-n junction. It produces neither a current nor a voltage.

Thus, the diode determines the I–Vcharacteristics of the cell. For this paper, the electrical equivalent circuit of a solar cell is shown in Fig. 1

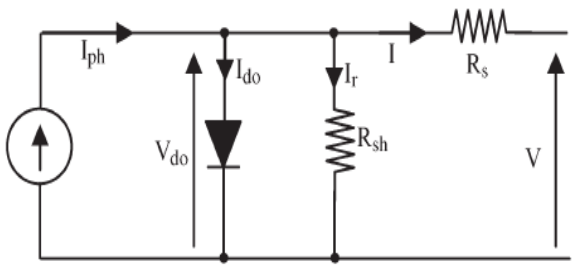

Fig.1. Solar cell electrically equivalent circuit.

A. characteristics of PV array:

The PV array – characteristic is described by the following [9]:

—— (1)

In (1), is the unit charge, the Boltzmann's constant, the p-n junction ideality factor, and T_c the cell temperature. Current $i_{rs}$is the cell reverse saturation current, which varies with temperature according to

— — — – (2)

In (2), T_{ref} is the cell reference temperature, the reverse saturation current at $T_{ref}$and E_G the band-gap energy of the cell. The PV current i_{ph} depends on the insolation level and the cell temperature according to

(3)

In (3), i_{scr} is the cell short-circuit current at the reference temperature and radiation, K_v a temperature coefficient, and the insolation level in kW/m . The power delivered by the PV array iscalculated by multiplying both sides of (1) by v_{pv}.

—— (4)

Substituting i_{ph} from (2) in (3), P_{pv} becomes

0

—— (5)

Based on (5), it is evident that the power delivered by the PV array is a function of insolation level at any given temperature. Since the inverter employed in the PV system of this paper is of current-source type, the power-versus-current characteristic of the PV array has to be examined. Fig. 2 illustrates the power-versus-current characteristic of the PV array based on the parameters listed in the Appendix for insolation levels of 0.25, 0.5, and 1 kW/m. Fig. 2 shows that can be maximized by control of i_{pv}, based on an MPPT strategy [9].

A. DC-DC Converter

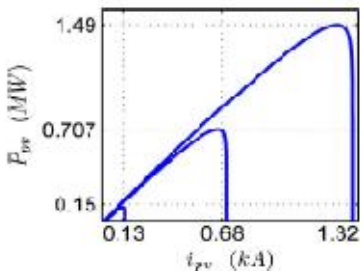

Fig. 2. P–I characteristic of a PV array for s=0.25, 0.5, and 1 kW/m².

III. STRUCTURE OF THE DG SYSTEM

Fig. 3 shows a diagram of the system used to analyze a typical connection of a DG system to a specific feeder, although studies to determine the best site for DG insertion should be performed before the operation analysis [7]. A power plant represents a secondary source (DG systems), while in this study the standard grid is a basic configuration system

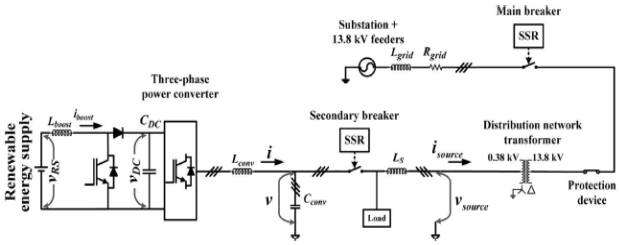

Fig. 3.Distributed generation system.

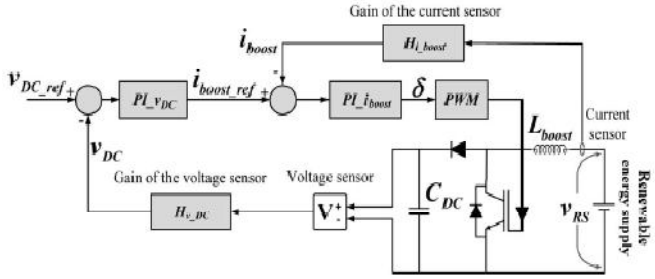

Fig. 4.Dc voltage/current control.

found in 1547 standard (simulated system) [23]. Furthermore, the primary energy used in the proposed DG system is the same as the previously mentioned renewable energy sources.

A dc-dc converter is employed to equalize the dc link voltage and deliver energy for fast transients when required by the local load, while a dc-ac converter is used to guarantee the power quality delivered to customers (local load) and the specific feeder. To avoid disturbances between the dc-ac converter and the feeder, a phase-locked loop (PLL) algorithm [11] associated with the zero voltage crossing detectors was used [24], [25].

A dc-dc step-up converter was used as an interface between the dc source and dc link of the three-phase dc-ac converter, as shown in Fig. 4. The step-up converter boosts the dc voltage and supplies the fast transients of energy required for the local load, thereby minimizing disturbances in the feeder current. The behavior of the step-up converter is similar to a voltage source, and the power it delivers to the grid depends on the point of maximum power (PMP) defined by the dc source [1]. The PMP is obtained using a tracking algorithm, based on the primary energy source. To keep the converters operating in a stable mode, proportional-integral (PI) controllers were used as a control technique to stabilize the *Lboost* current and dc voltage (*vDC*).

TABLE I
PI CURRENT PARAMETERS OF THE DC-DC CONVERTER

F_{CL}(Hz)	mf (°)	V_{DC}(v)	L_{boost} (mH)	Hi_boost
400	80	1000	5	1/250

TABLE II
PI VOLTAGE PARAMETERS OF THE DC-DC CONVERTER

F_{CL}(Hz)	mf (°)	V_{DC}(V)	C_{DC}(mF)	H_{v_DC}
50	60	1000	12	1/1500

A method based on phase-margin (*mf*) and cutoff frequency (*FCL*) was used to obtain the PIs constants (6) and (7) [2], [16], where the open loop gain (*GOL*), angular frequency (ω_{FCL}), and *mf* define the PIs constants (*kprop* and *kint*) [16].

(6)

(7)

B. DC-AC Converter

Closed-loop controls of the output current and voltage were implemented to guarantee inverter voltage quality. PI controller were also used as the control technique, while the design method of these PIs is the same as that used in the dc-dc step-up converter [16].

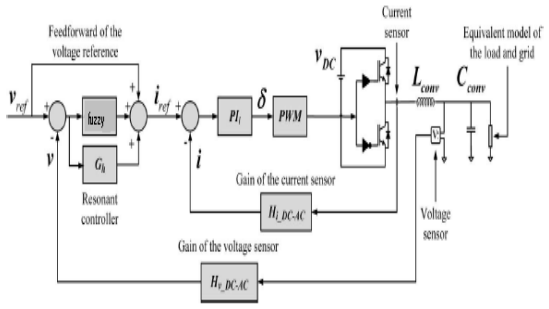

Fig. 5. Ac voltage/current control.

Since the closed-loop cutoff frequency of the PI current controller was chosen one decade below the switching frequency, the PI of the current retains a good compensation capability in the frequency range of interest. To improve this capability, a feed forward of the reference voltage could be used to compensate the residual error in the closed-loop gain at low frequencies. Due to its high power and the need for a reduced switching frequency, the voltage controller exhibits a low regulation bandwidth (a few hundred Hertz).

resonance angular frequency, and (*kih*) is the resonant controller gain [2], [11], [16]–[25].

A general block diagram demonstrating the control *v* is shown in Fig. 5. Where in ***Hi_DC−AC*** and ***Hv_DC−AC*** are the ac current and voltage sensors gains, respectively

(8)

C. Grid Characteristics

In the simulations, the complete distribution system found in 1547 standard [23] is composed of 13.8-kV feeders connected to a 69-kV radial line through 69/13.8-kV substation transformers, as shown in Fig. 5. To insert the DG at the distribution system, a 13.8/0.38 kV distribution network transformer is required to equalize the voltage levels.

TABLE IV
MODIFIED PARAMETERS OF THE CONVERTERS

V_{DC}(V)	C_{DC}(μF)	H_{v_DC}	H_{v_DC}	Hi_DC-AC
330	2800	1/12	1/360	1/12

The line model employed in the simulations took into account the Bergeron's traveling wave method used by the Electromagnetic Transients Program, which utilized wave propagation phenomena and line end reflections. Additionally, a set of switches was inserted between the DGs and distribution system, isolating them from each other to avoid the DG system supplies loads (loads placed in neighboring feeders where the DG was installed) connected to the high voltage side of the distribution transform. Due to the high level of power and voltage, 12 kHz was used as the PWM switching frequency for both converters.

An experimental setup was built to substantiate the DG operation. The grid was represented by a California Instruments LX 4500 source and an isolated 220/220-V transformer; the power converter was commanded by an Analog Devices 21992 DSP, while the parameters to design the controllers are those in Tables I–III except for the parameters in Table IV, which were calculated for a 3-kVA low scale prototype. To maintain their similarity with the simulations, the switching and sampling frequencies were also kept at 12 kHz.

The grid parameters (9) and (10) used in the experimental setup were calculated to have the same dynamic response as the simulated system. The main grid parameters of the equivalent model used in the experimental setup are represented by L_{grid}, R_{grid}, P_{SC}, f,

TABLE III
CURRENT PI PARAMETERS OF THE DC-AC CONVERTER

F_{CL}(Hz)	mf (°)	V_{DC}(V)	L_{conv}(mH)	H_{i_DC-AC}
1200	70	1000	2	1/250

To improve the control response of the output voltage regulator for fundamental and harmonic components, a resonant controller (8) is placed in parallel along with the PI controller, thereby reducing the converter impedance [16]. In (8),(*h*) is the harmonic order, (*ωch*) is the band pass around the resonance angular frequency, (*ω*0) is the and $V^2_{AB_{source}}$(inductance and resistance (losses), short circuit power, rated frequency, and rms voltage (phases A and B), respectively)

(9)

(10)

D. Synchronization Algorithm

To connect the DG to the grid, it is essential to synchronize both systems, which is done by means of a PLL algorithm that computes the average of the internal product between $v_{source}$and the synchronous voltage (v'_{λ}) [24]. If this equals zero in steady-state regime, $v'_{\lambda}$and v_{source} are perpendicular and synchronized [25]. The integration of the angular frequency (ω) then defines the θ angle ($\theta = wt$) used as the argument to produce v'_{λ}. Due to the high sampling and switching frequency $Ts \approx 0$, the delay block can be dismissed in the PLL closed loop transfer function

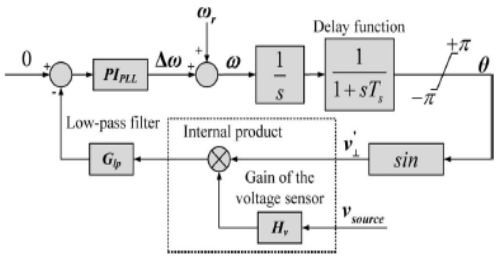

Fig. 6.PLL algorithm.

(11)

To compare the characteristic equation of the prototype transfer function with the PLL closed-loop transfer function (12), PI constants (13) and (14) can be adjusted by choosing the most suitable values for the natural undamped frequency (ωn) and damping ratio (ζ). To avoid stability problems, ωnshould ideally be greater than one or two periods of the fundamental frequency, and the maximum overshoot lower than 30%.

A general description of the PLL algorithm is found in Fig. 6, where ω_r, $\Delta\omega$, and $\boldsymbol{H}_v$are the rated angular frequency (= $2\pi 60$), adjusted angular frequency, and voltage sensor gain (1/360) (voltage measured at the grid), respectively

(12)

(13)

(14)

III. FEEDER CONTROL

Energy produced by the renewable energy sources can be transferred to the grid by controlling the amplitude of the voltage produced by the DG, and the angle between the grid voltage and the DG voltage (β angle) through a coupling inductor (L_S) [16], [18]. This serves as an additional inductance placed to connect the DG to the grid, or the leakage inductance of the DT. If *LS* is a DT parameter, v_{source}must be measured on the high voltage side of the distribution network transformer.

To achieve a controlled power flow from the DG to the grid, the DG voltage angle ($\boldsymbol{V}_A$) must be ahead of the grid voltage angle ($\boldsymbol{V}_{Asource}$). When this occurs, the DG delivers active power to the grid, as shown in Fig.7. The same analysis can be applied to the ac voltage amplitude produced by the DG: if the amplitude of $\boldsymbol{V}\,A$ is greater than $\boldsymbol{V}_{Asource}$the DG delivers reactive power to the grid; however, if the amplitude of $\boldsymbol{V}_A$is less than $\boldsymbol{V}_{Asource}$the DG absorbs reactive power from the grid.

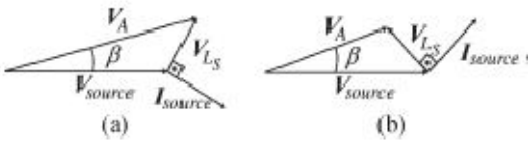

Fig. 7. Phasor diagrams. (a) Delivering active and reactive power. (b) Delivering active and absorbing reactive power.

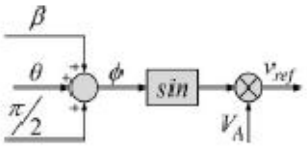

Fig. 8. Determination of the voltage reference.

The β angle is determined by the average power flowing to the grid (P_{source}), the connection reactance (X_{LS}), the rms phase voltage ($V_{Asource}$) synthesized by the grid, and the rms voltage produced (*VA*) by the DG according to (16). After defining the β angle, the DG voltage amplitude of $\boldsymbol{V}\,A$ must be adjusted, where $V_{Asource}$and *XLS* are the same parameters described in (10). If Q_{source}= 0 the unity power factor (PF) to the feeder is obtained [34]. Additionally, *LS* is designed for a small voltage variation on the ac local voltage produced by the dc-ac inverter [16].

In Fig. 8, the voltage reference (v_{ref}) of the dc-ac power converter is determined by displacing θ by $\pi/2$ and adding the β angle to the result. The φ angle is then used as the argument of a sinusoidal function and multiplied by *VA* to obtain the voltage reference that must be synthesized at the VSI terminals

(15)

(16)

V. SIMULATION ANALYSIS

Simulations were performed using MatLab/Simulink software, as shown in Fig. 3.

A. Connection and Power Transfer

Two procedures are required to connect the DG system to the feeder. First, an algorithm must be used to synchronize *vsource* with the voltage produced by the converter *v*. After synchronization, the algorithm to detect zero crossing of *vsource* must be initiated. When this is done, the switch connecting both systems is closed, minimizing the transient effects to the feeder (which occur up to 0.2 s).

Subsequently, a soft transfer (40kVA/s) of power starts at 0.25 s of the simulation range, followed by a base

load operation. Due to the method used synchronization and soft transfer of power minimal disturbances are observed in the grid, as shown in Figs. 9 and 10. However, when the soft transfer of power is completed, two groups of resistive loads are connected within a short time interval (one, demanding 70 kW, is inserted at 0.8 s; the other, demanding 60 kW, is connected at 1.3 s).Due to load capability, the current flowing through the grid inverts its direction, making additional power come from the grid. At the moment of the load connection, most of the electric variables are submitted to fast transients. However, this is not observed in the grid voltages because the short-circuit power of the grid is higher than the short-circuit power of the DG. To verify the power quality delivered to customers, total harmonic distortion (THD) of the DG voltage is well below 5%, whereas the PF is close to unity.

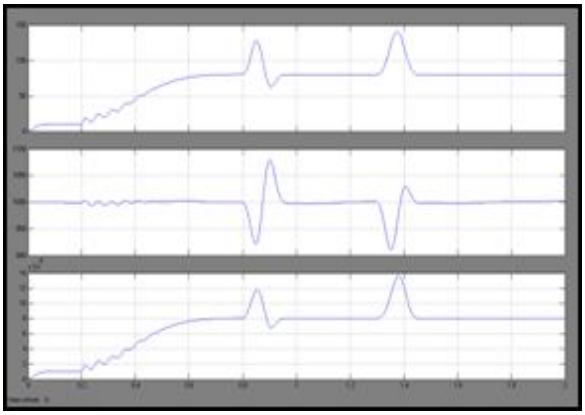

Fig. 9.Operation of the boost converter.

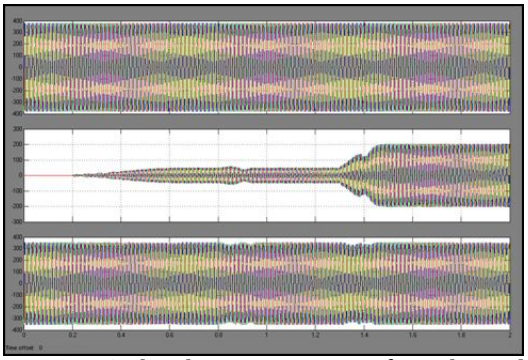

Fig. 10. DG absorbing active power from the grid.

B. Nonlinear Load

Another issue to be analyzed is the influence of a nonlinearload connected to the DG terminals. In this case, the controltechnique used to synthesize the ac voltage by the inverterplays an important role. In fact, it reduces the impedance ofthe inverter, making the DG system compensate the local loadharmonics. In this test, the load is inserted at 0.4 s and the DGis connected to the grid at 2 s, remaining so for 6 s.To observe the system's capability, the minimal value ofactive and reactive power flows through the grid, with the nonlinearload represented by a non-controlled three-phase powerrectifier plus *RC* load that demands around 50 kVA from the DG. In this operation mode, the THD of the voltage imposed by the VSI rises to 3%, even with the resonant controller compensating the 1st, 3rd, and 5th to 15th harmonics, however, the THD of the load current achieves more than 115%. To observe what happens with the DG system, a short time interval (1.96 to 2.04 s) before and after the connection with the grid is presented in Fig. 11, which demonstrates the DG capability to supply nonlinear loads in the connected or isolated modes.

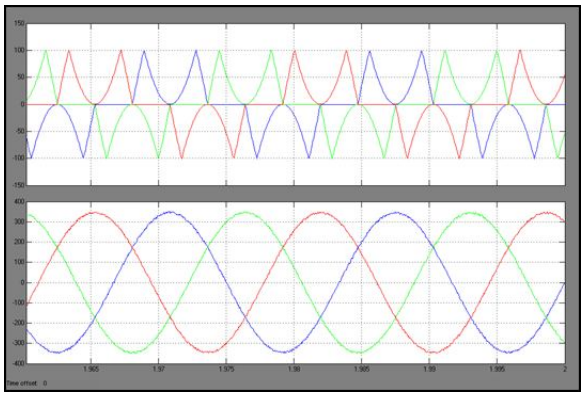

Fig. 11. Zoom of the load currents and voltages produced by the DG withnonlinear load.

C. Islanding Mode Consideration

When a short-circuit occurs on the high voltage side of theDT, the protection devices closest to the event disconnect thegrid from the distribution system in order to avoid stabilityproblems [35], [36]. However, the DG remains connected,forming a local area whose mode of operation may be dangerousif the local load demand is greater than the power producedby the DG. To avoid this, the DG must identify the contingencyas soon as possible and disconnect it from the local area.

To understand the effects on the grid and power converters,the following series of events was performed. First, a balancedthree-phase linear load demanding almost 25 kW was connectedto the DG terminals at the beginning of the simulation.

At 1.8 s, the power produced by the DG system was reduced(*pDC*drops from 125 kW to 100 kW), and a 75-kW threephaselinear load was connected to the DG terminals to obtaina minimal power level exchanged with the grid, which, asreported in literature [11], is the most difficult situation toidentify the islanding mode.

Fig. 12 identifies the effect of the islanding mode comparedwith the load connection or power transfer to the grid. In eachcase, the islanding mode did not affect the dc

link voltage andpower, or the ac power flow through the grid, which was not thecase for the load connection or power transfer.

D. Islanding and Reconnection to the Feeder

Another important aspect of the DG operation is the islandingmode followed by a reconnection. As above, the test at the beginning of the simulations, a balanced three-phase linear load demanding 30 kW was connected to the DG terminals. The power produced by the DG system was reduced from 125 kW to 90 kW, and a 25-kW three-phase linear local load was connected 1.25 s after the simulated range started.

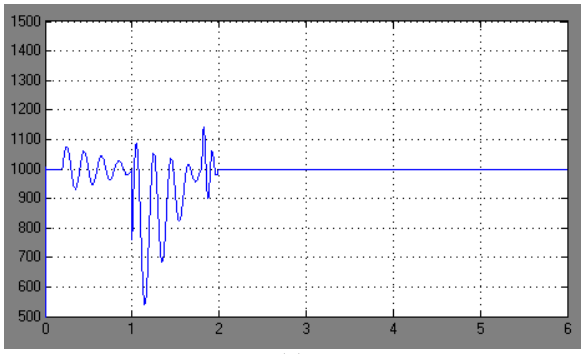

(a)

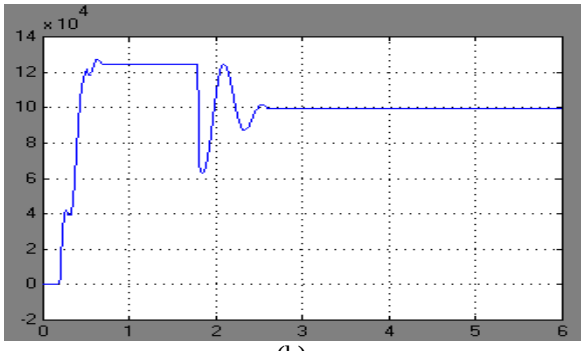

(b)

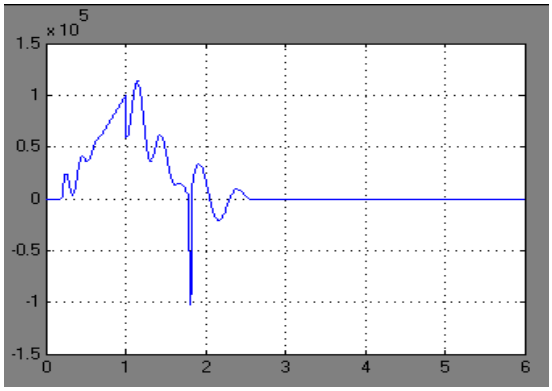

(c)

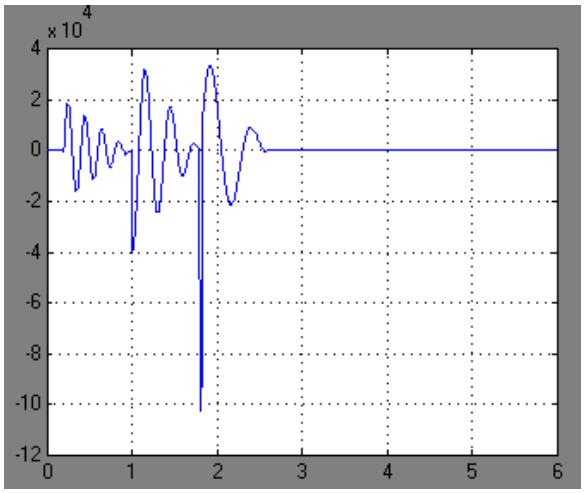

(d)

Fig. 12. Islanding with zero power flow

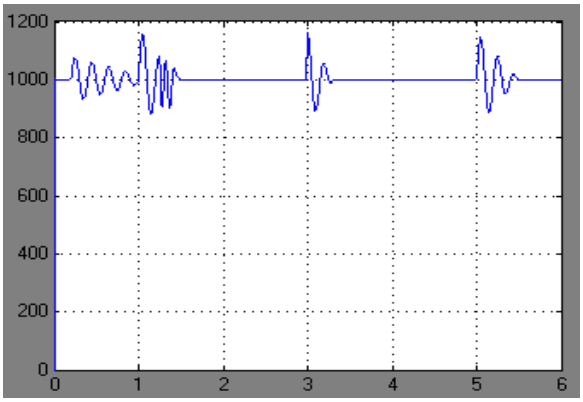

(a)

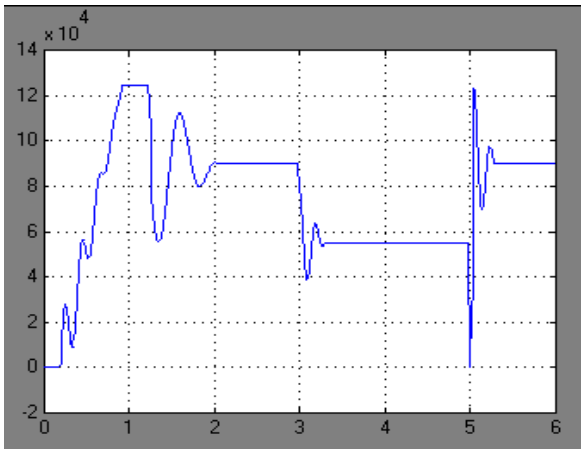

(b)

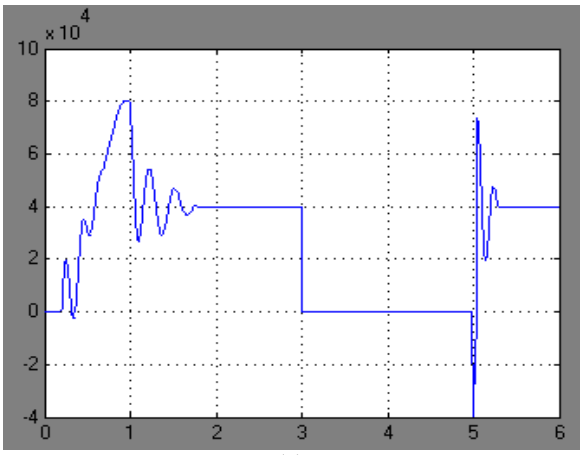

(c)

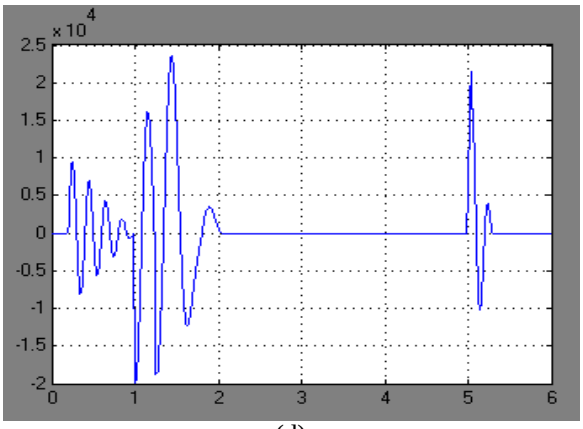

(d)

Fig. 13. Islanding and reconnection with nonzero power flow. Performed here considers a limited power level exchanged with the grid.

The DG voltage amplitude was subsequently adjusted to exchange −10 kVAr with the grid. This was undertaken to obtain a minimal level of active (35 kW) and reactive (−10 kVAr) power through the grid, as seen in Fig. 13. Unlike what occurred in Section III-C, the effects of islanding (at 3.0 s) followed by a reconnection [13] (at 5.0 s) were evident on the dc link voltage and power, or on the power flowing through the grid, with the most drastic case being the dc link power, which dropped to zero when the grid was reconnected.

VI. CONCLUSION

This paper proposes the operation of a 3-phase power connected to a distributed generation (DG) system with photovoltaic system. In This paper an alternative solution to connecting a DG system to the grid, whereby the amplitude and displacement of the voltage synthesized by the DG is regulated with respect to the grid voltage and the control variable before and after the contingency is always the same. Additionally, a dc-dc step-up converter and a dc-ac VSI are used in a DG system as an interface with the power grid. PI controller is associated with resonant regulators were used as a solution to produce distortion-free DG voltage, even when the local load is nonlinear or when distortion occurs in the grid voltage. Although the PLL algorithm tracks as rapidly as possible, the frequency oscillations are slowly damped due to the limits of amplitude.

REFERENCES

[1] M. G. Simões and F. A. Farret, *Integration of Alternative Sources of Energy*. Hoboken, NJ: Wiley, 2006.
[2] A. Keyhani,M. N.Marwali, andM. Dai, *Integration of Green and Renewable Energy in Electric Power Systems*. Hoboken, NJ: Wiley, 2010.
[3] S. Chowdhury, S. P. Chowdhury, G. A. Taylor, and Y. H. Song, "Mathematical modelling and performance evaluation of a stand-alone polycrystalline PV plant with MPPT facility," in *Proc. Power Energy Soc. Gen. Meeting—Conversion Delivery Electrical Energy 21st Century*, 2008, pp. 1–7.
[4] Y. Wen-Chih and H. Wei-Tzer, "A load transfer scheme of radial distribution feeders considering distributed generation," *Proc. CIS*, pp. 243–248, 2010.
[5] D. D. Marquezini, D. B. Ramos, R. Q. Machado, and F. A. Farret, "Interaction between proton exchange membrane fuel cells and power converters for AC integration," *IET Renewable Power Gener.*, vol. 2, no. 3, pp. 151–161, Sep. 2008.
[6] W. El-Khattam and M. M. A. Salama, "Distributed generation technologies, definitions and benefits," *Elect. Power Syst. Res.*, vol. 71, no. 2, pp. 119–128, Oct. 2004.
[7] A. Barin, L. F. Pozzatti, L. N. Canha, R. Q. Machado, A. R. Abaide, and G. Arend, "Electrical power and energy systems multi-objective analysis of impacts of distributed generation placement on the operational characteristics of networks for distribution system planning," *Int. J. Elect. Power Energy Syst.*, vol. 32, no. 10, pp. 1157–1164, Dec. 2010.
[8] S. Chaitusaney and A. Yokoyama, "Impact of protection coordination on sizes of several distributed generation sources," in *Proc. IPEC*, 2005, pp. 669–674.
[9] IEEE Recommended Practices and Requirements for Harmonic Control in Electrical Power Systems, IEEE Std. 519, 1993.
[10] Agância Nacional de Energia Elétrica—ANEEL, Procedimento de Distribuição de Energia Elétrica no Sistema Elétrico National— PRODIST—Módulo 32010.
[11] F. Blaabjerg, R. Teodorescu, M. Liserre, and A. V. Timbus, "Overview of control and grid synchronization for distributed power generation systems," *IEEE Trans. Ind. Electron.*, vol. 53, no. 4, pp. 1398–1409, Oct. 2006.

[12] J. M. E. Huerta, J. Castello-Moreno, J. R. Fischer, and R. Garcia-Gil, "A synchronous reference frame robust predictive current control for threephase grid-connected inverters," *IEEE Trans. Ind. Electron.*, vol. 57, no. 3, pp. 954–962, Mar. 2010.
[13] P. Rodriguez, A. V. Timbus, R. Teodorescu, M. Liserre, and F. Blaabjerg, "Flexible active power control of distributed power generation systems during grid faults," *IEEE Trans. Ind. Electron.*, vol. 54, no. 5, pp. 2583– 2592, Oct. 2007.
[14] T. Hornik and Z. Qing-Chang, "A current-control strategy for voltage source inverters in micro grids based on$H\infty$ and repetitive control," *IEEE Trans. Power Electron.*, vol. 26, no. 3, pp. 943–952, Mar. 2011.
[15] I. J. Balaguer, L. Qin, Y. Shuitao, U. Supatti, and P. F. Zheng, "Control for grid-connected and intentional islanding operations of distributed power generation," *IEEE Trans. Ind. Electron.*, vol. 58, no. 1, pp. 147–157, Jan. 2011.
[16] R. Q. Machado, S. Buso, and J. A. Pomilio, "A line-interactive singlephase to three-phase converter system," *IEEE Trans. Power Electron.*, vol. 21, no. 6, pp. 1628–1636, Nov. 2006.
[17] F. Gao, S. Member, and M. R. Iravani, "A control strategy for a distributed generation unit in grid-connected and autonomous modes of operation," *IEEE Trans. Power Del.*, vol. 23, no. 2, pp. 850–859, Apr. 2008.
[18] H. Kim, T. Yu, and S. Choi, "Indirect current control algorithm for utility interactive inverters in distributed generation systems," *IEEE Trans. Power Electron.*, vol. 23, no. 3, pp. 1342–1347, May 2008. [19] Agência Nacional de Energia Elétrica—ANEEL, Procedimento de Distribuição de Energia Elétrica no Sistema Elétrico Nacional—PRODIST—Módulo 82010.
[20] J. M. Guerrero, J. C. Vasquez, J. Matas, L. G. de Vicuna, and M. Castilla, "Hierarchical control of droop-controlled AC and DC microgrids—A general approach toward standardization," *IEEE Trans. Ind. Electron.*, vol. 58, no. 1, pp. 158–172, Jan. 2011.
[21] J. M. Guerrero, J. Matas, L. G. de Vicuna, M. Castilla, and J. Miret, "Wireless-control strategy for parallel operation of distributed-generation inverters," *IEEE Trans. Ind. Electron.*, vol. 53, no. 5, pp. 1461–1470, Oct. 2006.
[22] J. M. Guerrero, J. Matas, V. L. Garcia de, M. Castilla, and J. Miret, "Decentralized control for parallel operation of distributed generation inverters using resistive output impedance," *IEEE Trans. Ind. Electron.*, vol. 54, no. 2, pp. 994–1004, Apr. 2007. [23] Standard for Interconnecting Distributed Resources With Electric PowerSystems, IEEE Std. 1547, 2003.
[24] F. P. Marafão, S. M. Deckmann, J. A. Pomilio, and R. Q. Machado, "Metodologia de projeto e análise de algoritmos de sincronismo PLL," *SOBRAEP Revista da Associação Brasileira de Eletrônica de Potência*, vol. 10, no. 1, pp. 7–14, 2005.
[25] V. Kaura and V. Blasko, "Operation of a phase locked loop system under distorted utility conditions," *IEEE Trans. Ind. Appl.*, vol. 33, no. 1, pp. 58– 63, Jan./Feb. 1997.

N UMAKAMESHWARI DEEPIKAcurrently pursuing her M.Tech in Electrrical Power systems from VIGNAN BHARATHI INSTITUTE OF TECHNOLOGY, affiliated to JNT University, Hyderabad. She has done her B.Tech degree in 2009 from UNIVERSITY COLLEGE OF ENGINEERING, KAKATIYA UNIVERSITY, KOTHAGUDEM and her fields of interest include Power System and Electrical machines.

M/S J. ARCHANA has completed her B.Tech Electrical & Electronics Engineering in 2007 from ADAMS ENGINEERING COLLEGE, affiliated to JNTUH. M.TECH in Power electronics and electric drives in 2009 from G.NARAYANAMMA INSTITUTE OF TECHNOLOGY, affiliated to JNTUH University, and presently she is working as Assistant Professor in EEE department at Vignan Bharathi Institute of technology, Ghatkesar, Telangana, India. Her area of interest includes power systems and power electronics.